Malaysian Journal of Analytical Sciences (MJAS)
Published by Malaysian Analytical Sciences Society

NANOPARTICLES FUNCTIONALIZED REDUCED GRAPHENE OXIDE THIN FILMS FOR DETECTION OF ACETIC ACID AT LOW CONCENTRATIONS

(Filem Nipis Grafin Oksida Terkurang Berfungsi Nanopartikel untuk Pengesanan Asid Asetik pada Kepekatan Rendah)

Nor Syahira Mohd Tombel[1*], Marmeezee Mohd Yusoff[2], Hasan Firdaus Mohd Zaki[2,3], Firzalaila Syarina Md Yakin[4] and Siti Aishah Mohamad Badaruddin[5]

[1]Department of Computational and Theoretical Sciences, Kulliyyah of Science, International Islamic University of Malaysia, 25200, Kuantan, Pahang, Malaysia
[2]Kulliyyah of Engineering, International Islamic University Malaysia, Jalan Gombak, 53100, Kuala Lumpur, Malaysia
[3]Centre for Unmanned Technologies (CUTe), Kulliyyah of Engineering, International Islamic University of Malaysia, Jalan Gombak, 53100, Kuala Lumpur, Malaysia
[4]Advanced Devices Lab, MIMOS Berhad, Technology Park Malaysia, 57000 Kuala Lumpur, Malaysia

[*]Corresponding author: norsyahiramt@gmail.com

Received: 31 January 2022; Accepted: 23 April 2022; Published: 27 December 2022

Abstract

This research proposes reduced graphene oxide (rGO) functionalized with nanoparticles (NPs) from gold (Au), silver (Ag) and platinum (Pt) as a sensing material for the detection of acetic acid gas at low concentrations, from 1 to 5 part per million (ppm). The rGO was functionalized with NPs at different sputtering durations (15 sec and 75 sec) and relative frequency (RF) power (30W and 70W) to study the enhancement of sensing properties. The sensors were exposed to acetic acid from 1 to 5 ppm in the presence of 20% relative humidity (RH) and at 30 °C room temperature. In this work, the Au NPs/rGO (30W 15s), Ag NPs/rGO (30W 15s) and Pt NPs/rGO (70W 15s) sensors were reported to have a good response with sheet resistance, (R_s) at values: 327.2, 453.844 and 201.084 Ω/sq, respectively, compared with the reference sensor, rGO at only R_s, 529.614 Ω/sq. The three sensors had also recorded high R^2 values compared to the reference rGO (0.9448) with values of 0.993, 0.966 and 0.995 for Au/rGO (30W 15s), Ag/rGO (30W 15s) and Pt/rGO (70W 15s), respectively. Thus, the functionalization of rGO with nanoparticles can enhance the sensor's electrical properties and generate good responses for acetic acid gas detection at low concentrations.

Keywords: reduced graphene oxide, functionalization, nanoparticle, response, sensitivity, gas detection.

Abstrak

Penyelidikan ini mencadangkan grafin oksida terkurang (rGO) dan kefungsiannya dengan nanopartikel (NPs) daripada emas (Au), perak (Ag) dan platinum (Pt) sebagai bahan penderiaan untuk pengesanan gas asid asetik pada kepekatan rendah. NPs telah difungsikan dengan rGO pada tempoh percikan yang berbeza (15 saat dan 75 saat) dan kuasa frekuensi relatif (RF) (30W dan 70W) untuk mengkaji peningkatan sifat penderiaan peranti penderia. Penderia didedahkan dengan asid asetik dari 1 hingga 5 bahagian per juta (ppm) kepekatan dengan kehadiran 20% Kelembapan Relatif (RH) dan pada suhu bilik 30 °C. Dalam kerja ini, penderia Au NPs/rGO (30W 15s), Ag NPs/rGO (30W 15s) dan Pt NPs/rGO (70W 15s) dilaporkan mempunyai tindak balas yang baik dengan nilai rintangan lembaran, Rs yang diukur; 327.2, 453.844 dan 201.084 Ω/sq, masing-masing, dengan nilai yang lebih rendah daripada penderia rujukan, rGO sahaja iaitu 529.614 Ω/sq. Ketiga-tiga penderia itu juga mencatatkan nilai R^2 yang lebih tinggi berbanding rGO rujukan (0.9448) dengan nilai masing-masing 0.993, 0.966 dan 0.995 untuk Au NPs/rGO (30W 15s), Ag NPs/rGO (30W 15s) dan Pt NPs/rGO (70W 15s). Oleh itu, kefungsian rGO dengan nanopartikel boleh meningkatkan sifat elektrik sensor dan menjana tindak balas yang baik untuk pengesanan gas asid asetik pada kepekatan rendah.

Kata kunci: grafin oksida terkurang, kefungsian, nanopartikel, tindak balas, kepekaan, pengesanan gas

Introduction

Graphene is a two-dimensional crystalline material that has become a promising sensing element due to its unique properties of having high surface area [1], fast electrical transport, zero bandgap semiconductor [2] and high electron mobility at room temperature [3]. The properties of graphene demonstrate its potential for gas sensing applications with high sensitivity, which is mainly related to the resistivity and adsorption sites of the surface material.

Graphene oxide (GO) and reduced graphene oxide (rGO) derived from graphene can further improve the performance of a material as a sensing element [4]. GO and rGO have good electrical conductivity and sensitive surface adsorbates compared to graphene only due to the crystal defects and oxygen functionalization on its edge and basal [5-6]. A large number of functional groups and defects on rGO provide abundance adsorption sites [7]. Metal oxide nanoparticles such as gold (Au), silver (Ag) and platinum (Pt) have been functionalized with graphene or rGO to enhance the sensitivity of the surface material. Metal nanoparticles are reported to be an excellent catalyst due to their high ratio of surface atoms which increase the subsequent interaction of targeted gases with the absorbed oxygen species on the sensing surface [2,8].

In the medical field, the detection of a volatile organic compound (VOC) through breath analysis has been used as a quick and non-invasive diagnostic procedure to monitor human health. There are hundreds of VOCs used as preclinical biomarkers in diagnosing various pulmonary diseases as they are linked to metabolic activity in the body and provide information about an individual's health [9]. Many gasses were studied for VOC detection such as acetone, toluene, isoprene, acetaldehyde, ethanol, acetic acid, phenol and 2-propanol [10-11]. Acetic acid is a natural biomarker that is correlated with metabolic acids. It is an indicator of airways acidification for a patient with gastroesophageal reflux and cystic fibrosis disease [12]. Thus, a non-invasive approach for the detection of VOC as a breath biomarker is expected to improve health monitoring and early diagnosis [9].

In this study, we report the functionalized rGO with Au NPs, Ag NPs, and Pt NPs as a thin film on resistive VOC sensors for acetic acid detection. Different sputtering durations and powers during the deposition of the nanoparticle on the rGO thin film were tested to study the consequences on the sensing properties. The electrical parameters of the sensing materials, such as sheet resistivity and conductivity, were measured using hall effect measurement. Furthermore, the sensor sensing behavior was determined and studied from the detection of acetic acid gas (1 to 5 ppm) in the presence of 20% relative humidity (RH) at room temperature. The result from this study highlights the material that has suitable fabrication parameters with good performance and sensitivity to low concentrations of acetic acid at room temperature.

Materials and Methods

The rGO was derived from GO films as mentioned in [12]. The rGO layer was spin-coated and reduced at a

temperature of more than 700 °C. Then, the rGO was patterned as sensing material on top of a titanium/platinum (Ti/Pt) interdigitated electrode (IDE) that was deposited on a silicon dioxide/silicon (SiO_2/Si) substrate. The sensor was then loaded into a vacuum deposition chamber for Au NPs (99.99% purity) and sputtered at the duration of 15 sec and 75 sec. The sputtering was carried out in an Ar environment at 0.005 mbar with RF power of 30W and 70W. The lift-off process was done by soaking the sensors in acetone solutions where the photoresist on pads was removed. This process was repeated for Ag and Pt nanoparticles functionalization. The sensor's design is illustrated in Figure 1 and the details of the parameter are described in Table 1.

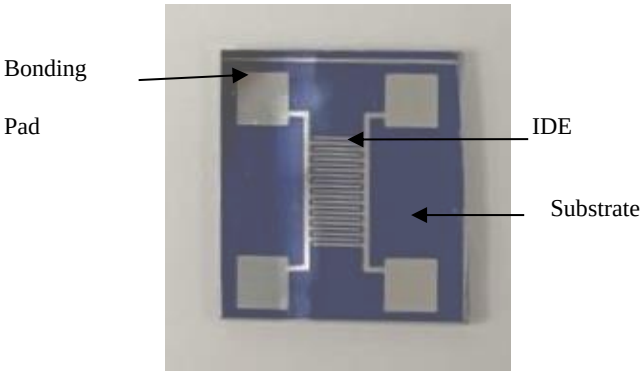

Figure 1. Image of the VOC sensor

Table 1. List of Samples and Parameters of the VOC Sensors

Sample No.	Nanoparticles	Power (WRF)	Time (sec)	Remarks
1	Reference rGO film			Bare rGO
2	Au	30	15	Au NPs/rGO (30W 15s)
3	Au	30	75	Au NPs/rGO (30W 75s)
4	Au	70	15	Au NPs/rGO (70W 15s)
5	Au	70	75	Au NPs/rGO (70W 75s)
6	Ag	30	15	Ag NPs/rGO (30W 15s)
7	Ag	30	75	Ag NPs/rGO (30W 75s)
8	Ag	70	15	Ag NPs/rGO (70W 15s)
9	Ag	70	75	Ag NPs/rGO (70W 75s)
10	Pt	30	15	Pt NPs/rGO (30W 15s)
11	Pt	30	75	Pt NPs/rGO (30W 75s)
12	Pt	70	15	Pt NPs/rGO (70W 15s)
13	Pt	70	75	Pt NPs/rGO (70W 75s)

***rGO= reduced graphene oxide, Au NPs = Gold nanoparticle, Ag NPs = Silver nanoparticle, Pt NPs = Platinum nanoparticle**

The electrical properties of the sensors were obtained using hall effect measurement (Ecopia HMS-5300) at room temperature before proceeding with the VOC gas detection test. The experimental setup for the gas sensing system is illustrated in Figure 2. The procedure was the same as mentioned in the previous study [13].

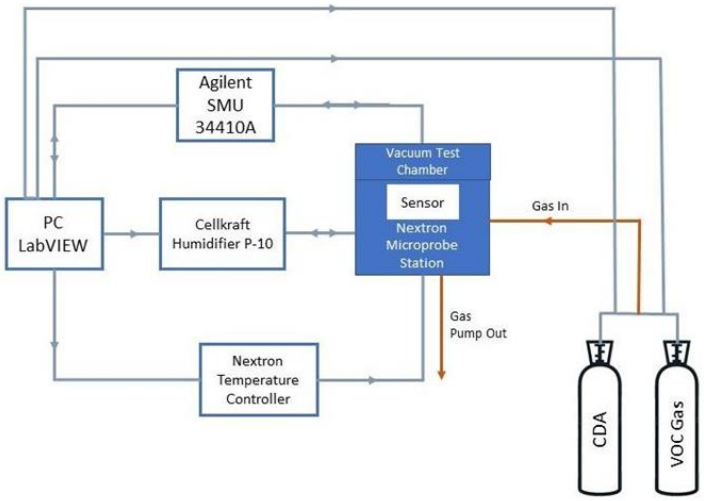

Figure 2. Schematic diagram of the experimental setup for gas detection system

The sensor was put on a sample stage in the Nextron microprobe station. Then, gas testing measurement was applied with a clean exposure method at 20% RH and at room temperature, 30℃. The flow of clean dry air (CDA) was maintained at 1 L/min for 3 min to stabilize the baseline reading for the sensor. Next, the VOC gas was exposed to the sensor at 1ppm for 30 sec. Then, the gas purged out and the CDA was allowed to flow again in 30 sec. The method was repeated by increasing the gas concentration with 1 to 5 ppm. Changes in resistance reading as the signal output were used to measure the sensor response and sensitivity (S) using the formula below [14, 15]:

$$\Delta R = R_{air} - R_{gas} \quad (1)$$

$$\text{Sensitivity (S)} = R_{air}/R_{gas} \quad (2)$$

$$\text{Response} = \frac{\Delta R}{R_{gas}} \times 100\ (\%) \quad (3)$$

Where R_{air} is an average resistance in CDA only, without VOC gas. R_{gas} is an average resistance with the exposure of VOC gas.

Results and Discussion

Surface morphology

Figure 3 shows the FESEM images of rGO thin film sputtered with Au NPs/rGO, Ag NPs/rGO and Pt NPs/rGO for parameters 30W 15 sec, 30W 75 sec, 70W 15 sec and 70W 75 sec with 200k applied magnification for each device. Based on Figure 3, the grain size was increased with the increase of time and power. Good particle formation can be found at 15 sec to 75 sec duration of nanoparticle sputtering. The nanoparticle size for Au and Ag had become bigger as the power and sputtering duration increased. Meanwhile, the grain size for Ag NPs/rGO at 70W began to agglomerate into large entities and become irregular in shape. This may be due to the coalescence of nanoparticles at a longer sputtering duration [16]. Pt NPs still showed a smaller size at 30W and 70W, and the grain size cannot be seen clearly as it was fully deposited onto the rGO thin film compared with Au and Ag NPs.

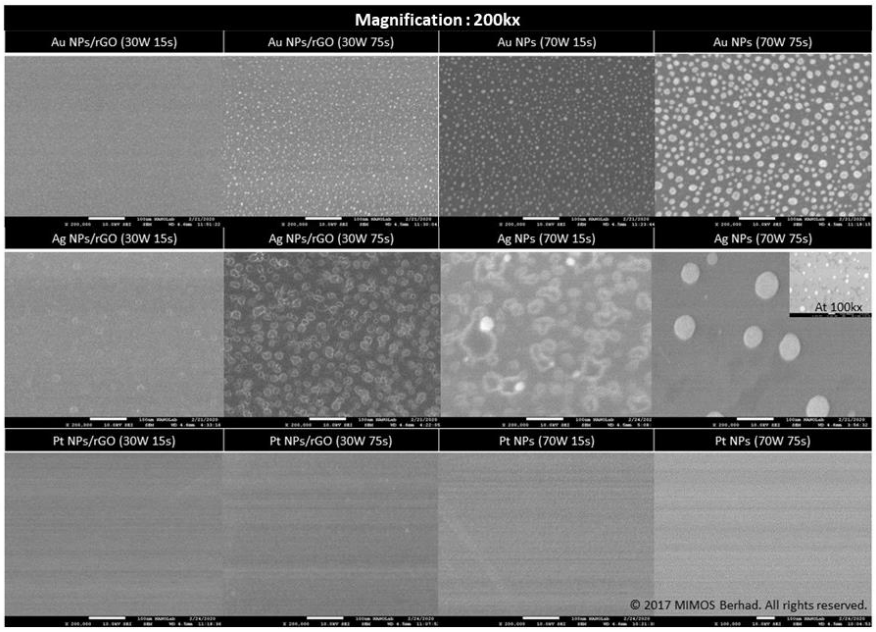

Figure 3. FESEM image of nanoparticle Au, Ag and Pt on rGO thin film after 15 sec and 75 sec sputtering at 30W and 70W

Hall effect measurement analysis

Electrical properties such as average sheet resistivity, Rs, average resistance, R and conductivity, σ of thin film on the samples were obtained from the hall effect measurement and are listed in Table 2. Functionalized NPs except Ag NPS/rGO at 70W had shown lower resistivity compared with the reference sensor, the thin film with rGO only. The NPs' functionalization on the rGO thin film was varied with power and sputtering duration. The variation caused defect concentrations on the thin film and increased the electrical properties of NPs functionalized rGO rather than the thin film of the rGO only [17].

Table 2. List of electrical properties for the VOC sensor

Sensor	Average Resistance Sheet, Rs, (Ω/sq)	Average Resistance, R (Ω)	Conductivity, σ (S/cm)
rGO	529.61	0.000201	4964.56
Au NPs/rGO (30W 15s)	327.20	0.000129	7732.44
Au NPs/rGO (30W 75s)	394.16	0.000154	6475.38
Au NPs/rGO (70W 15s)	394.43	0.000155	6471.26
Au NPs/rGO (70W 75s)	394.84	0.000154	6497.20
Ag NPs/rGO (30W 15s)	453.84	0.000176	5689.86
Ag NPs/rGO (30W 75s)	467.94	0.000181	5518.76
Ag NPs/rGO (70W 15s)	793.39	0.000300	3331.94
Ag NPs/rGO (70W 75s)	3641.00	0.001364	733.388
Pt NPs/rGO (30W 15s)	270.02	0.000109	9163.50
Pt NPs/rGO (30W 75s)	286.96	0.000116	8595.58
Pt NPs/rGO (70W 15s)	201.08	0.000085	11758.20
Pt NPs/rGO (70W 75s)	426.37	0.000166	6032.040

Figure 4 plots the average sheet resistivity, R_s value for Au NPs/rGO, Ag NPs/rGO and Pt NPs/rGO films at the different parameters. The bare rGO film marked as a reference sensor has a R_s value of 529.61 Ω/sq. Meanwhile, for rGO functionalized with Au, Ag and Pt, the NPs showed a decrease in the Rs value except for Ag NPs at 70 W. The sensor with thin film Au NPs/rGO, Ag NPs/rGO and Pt NPs/rGO at 30W and 15 sec had the R_s value decrease to 327.2, 453. 84 and 270.02 Ω/sq, respectively. However, Ag NPs/rGO at 70W at sputtering time 15 sec to 75 sec showed a gradual increase in the sheet resistivity from 793.39 Ω/sq to 3641.00 Ω/sq, which may be due to the increment of the grain size for Ag NPs at high power. The increment of power and sputtering time during functionalization had increased the grain size of the NPs (refer to Figure 3), thus increasing the sheet resistivity of the thin film. The increased grain size of the nanoparticle had affected the resistivity of the device as the grain boundaries act as scattering centers for the electron [18].

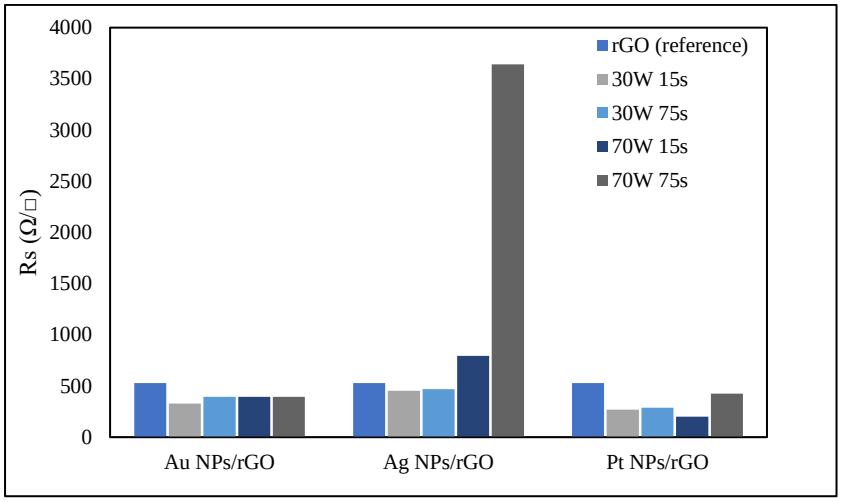

Figure 4. The sheet resistivity of the rGO and the functionalization with nanoparticles at four different parameters

Sensor response measurement

The response from the reference sensor during exposure to acetic acid is shown in Figure 5. At first, when the CDA was exposed to the chamber, the resistance increased due to the removal of electrons that took place by oxygen absorption in the depletion layer. At this phase, the sensor also showed a drift in baseline reading. Drift in sensor response occurs due to many factors, such as the age of the sensor or variation from environmental conditions. For this sensor, the source of the sensor drift may come from the temperature or humidity changes in the chamber [19].

Next, when the acetic acid was purged into the chamber, resistance from the rGO sensing layer began to decrease. This is because the gas molecules reacted with the adsorbed oxygen ions and the electrons were absorbed back into the conduction band [17]. The sensor with rGO and NPs functionalized rGO acted as an n-type semiconductor. Thus, the resistance decreased as the acetic acid acted as a reducing gas on the sensing element.

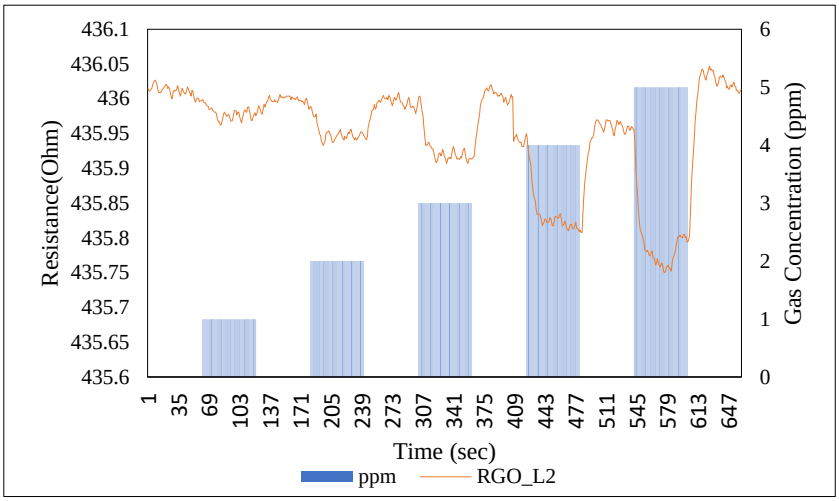

Figure 5. Response rGO thin film-based VOC Sensor on 1 to 5 ppm of acetic acid

Figure 6 shows the average sensitivity for functionalized rGO with a) Au NPs, b) Ag NPs and c) Pt NPs. The sensitivity of the sensor increased as the concentration increased. Meanwhile, Figure 7 showed the R^2 value for the linearity of the sensor response that corresponds with the gas concentration. For sensor selection, the sensor response and the R^2 value were compared for each sensor.

Based on the result in Figure 6a, the Au NPs/rGO sensors had low sensitivity with acetic acid compared with the reference sensor. However, the linearity of the sensor response based on Figure 7 showed that Au NPs/rGO at 30W and 15 sec had R^2 value 0.9869, which was the highest among the others, followed by Au NPs/rGO at 70W and 75 sec. The sheet resistivity for Au NPs was also the lowest at 30W and 15 sec at 327.20 Ω/sq. The sensor conductivity for Au NPs at 30W reached maximum at low sputtering duration, while at high sputtering duration, it was good at high power.

Next, for Ag NPs functionalization, parameter 70W and 75 sec showed a good response compared to the reference sensor. Even though the Ag NPs/rGO (70W 75s) sensor had the highest R_s with 3641 Ω/sq, the sensitivity of the sensors was higher based on the result in Figure 6b. The sensitivity of the Ag NPs functionalized rGO was higher than pure rGO because the attachment of the Ag nanoparticle onto the rGO led to more active sites such as defects and oxygen functional group for adsorption of VOC molecules [20]. Besides that, the agglomerate grain size of Ag NP on the rGO thin film caused it to become more sensitive with the acetic acid. Based on Chen Zhou et al. in their study in 2012, a decrease in the grain size of the nanoparticle on the thin film was reported to be low in electrical and thermal conductivities [21].

Next, for the Pt NPs/rGO sensor in Figure 6c, the sensitivity with the acetic acid was the same as Au NPs which is lower than the pure rGO. The grain size of the nanoparticle can be seen clearly as Ag NPs, however the R^2 value for the Pt NPs/rGO sensor at high power (70W) had a high R^2 value compared to the pure rGO and Pt NPs/rGO at 30W. Based on the hall effect measurement, Pt NPs had low R_s value compared to the pure rGO. However, a good linearity of the sensor response was observed at high power for Pt NPs at 15 sec and 75 sec with 0.9948 and 0.9842, respectively. The Rs value for Pt NPs/rGO at 30W 15 sec had increased from 270.02 to 286.96 Ω/sq. The lowest R^2 value for the Pt NPs at low power can be affected by the duration of sputtering. Pt is commonly used as an electrode as it has high chemical stability and is more stable at high temperature [17], thus, the sensor's sensitivity can be seen as good at high temperature.

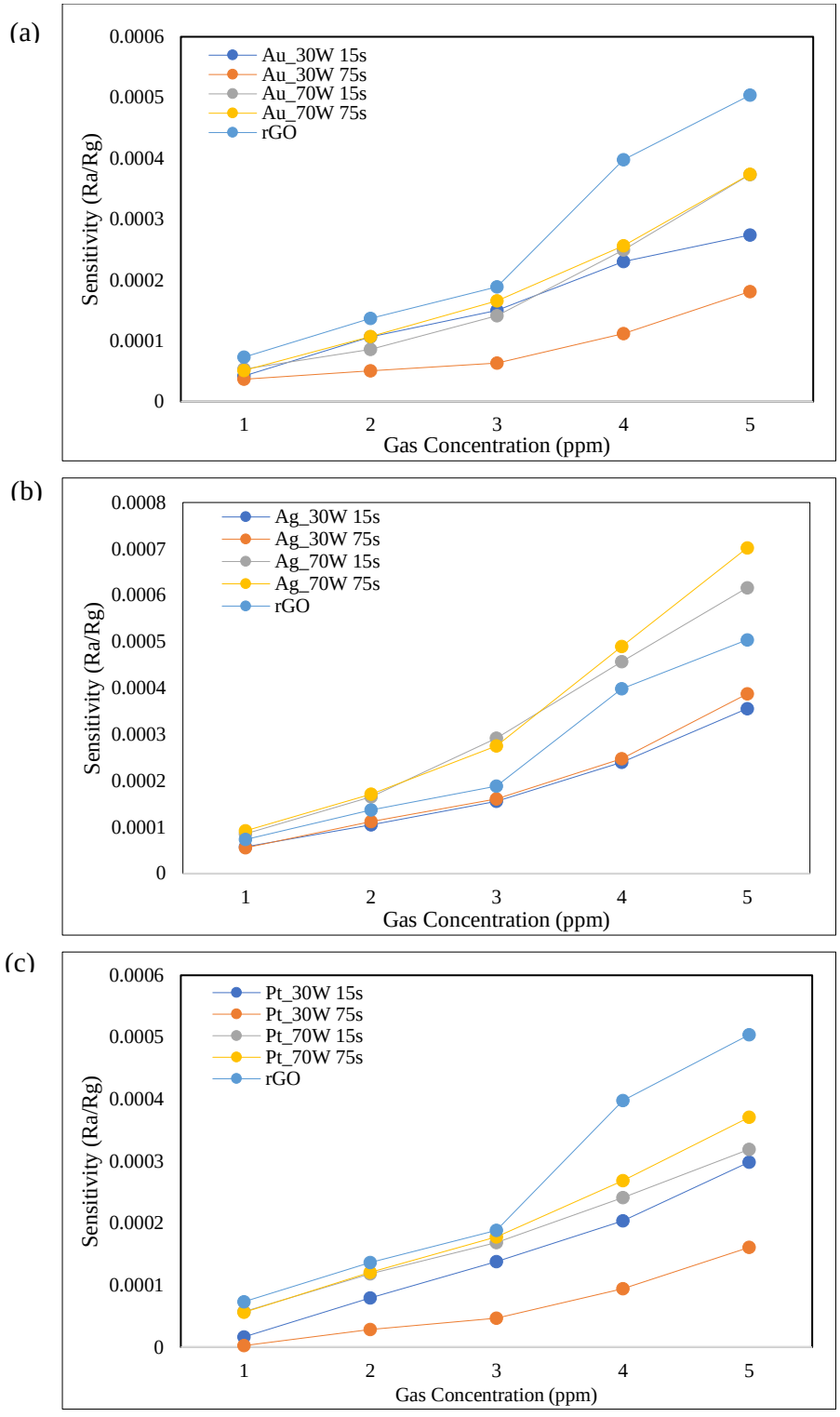

Figure 6. Sensitivity for functionalized rGO with a) Au NPs, b) Ag NPs and c) Pt NPs sensors

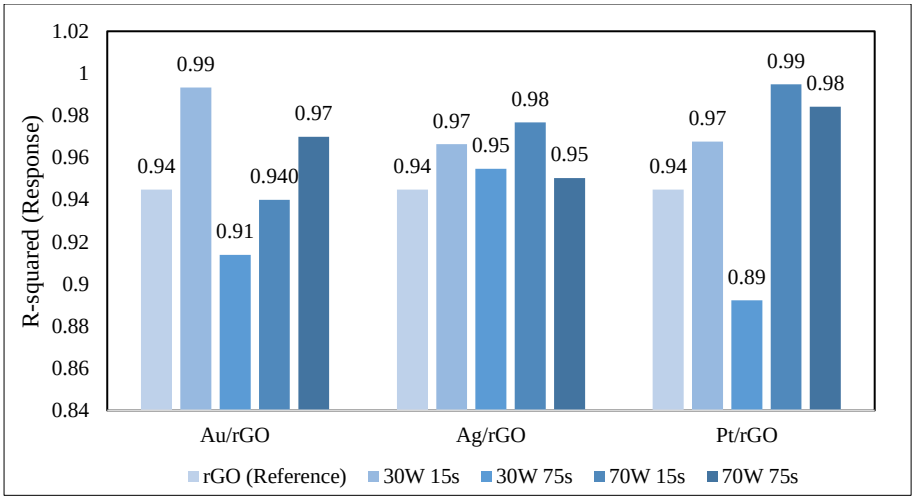

Figure 7. The R^2 value for the sensors on the detection of acetic acid

Conclusion

In this work, the n-type material was separately analyzed to detect reducing gas. The VOC sensors of rGO functionalized with NPs can detect low concentrations of acetic acid at a low operating temperature. The sensitivity results were compared between metal nanoparticles at different powers and durations. However, the cause of sensitivity for different types of nanoparticle functionalization rGOs were affected by different reasons. For Au NPs, the sensitivity of the sensor was influenced by the resistivity of the thin film, while for Ag NPs, the agglomerate of the grain size was more affected. For Pt NPs, high power made the sensor more sensitive to acetic acid. Hence, the study for these sensors can be taken further by varying the sputtering duration at each power and comparing it with more types of gas so that the effect of the nanoparticle on rGO thin film can be understood better and thus can be used for sensor selection.

Acknowledgement

This project is a collaboration between the International Islamic University Malaysia (IIUM) with the Centre of Unmanned Technologies, Kulliyyah of Engineering and Department of R&D, MIMOS Bhd. This research was partially sponsored by the Fundamental Research Grant Scheme (FRGS19159-0768) and MIMOS Berhad (SPG21-015-0015). We thank Dr. Ismahadi Syono for the main supervision.

References

1. Zhang, H., Li, Q., Huang, J., Du, Y. and Ruan, S. C. (2016). Reduced graphene oxide / Au Nanocomposite for NO_2 sensing at low operating temperature. *Sensor,* 16(2): 1-9.
2. Abdel-Karim, R., Reda, Y. and Abdel-Fattah, A. (2020). Review: Nanostructured materials-based nanosensors. *Journal of The Electrochemical Society,* 167: 037554.
3. Paula, M., Gil, G., Sandra, C., Nuno, A., Manoj, S., Jos, G. and Antnio, S. (2017), Functionalized graphene nanocomposites. *Advances in Nanocomposite Technology,* 2017: 11-15.
4. Behi, S., Bohli, N., Casanova-ch, J. and Llobet, E. (2020). Metal oxide nanoparticle-decorated few layer graphene nanoflake chemoresistors for the detection of aromatic volatile organic compounds. *Sensors,* 20: 3413:1-15.
5. Lipatov, A., Varezhnikov, A., Wilson, P. and Sysoev, V. V. (2013). Highly selective gas sensor arrays based on thermally reduced graphene oxide. *Nanoscale,* 5: 5426-5434.

6. Abdullah, M. F., Soriadi, N., Yakin, F.S.M, Badaruddin, S.A.M. and Syono, M. I. (2020). Materials science in semiconductor processing tuning the optoelectronic properties of the rGO-AuNPs hybrid film by pre-decoration and AuNPs-assisted thermal reduction. *Materials Science in Semiconductor Processing,* 112: 105017.
7. Wang, C., Lei, S., Li, X., Guo, S., Cui, P., Wei, X., Liu, W. and Liu, H. (2018). A reduced GO-graphene hybrid gas sensor for ultra-low concentration ammonia detection. *Sensors (Switzerland),* 18(9): 3147.
8. Mirzaei, A., Lee, J., Majhi, S. M., Weber, M., Bechelany, M. and Kim, H. W. (2019). Resistive gas sensors based on metal-oxide nanowires Resistive gas sensors based on metal-oxide nanowires. *Journal of Applied Physics,* 2019: 241102.
9. Malika, K., Kim, T., Losic, D. and Thanh, T. (2016). Recent advances in engineered graphene and composites for detection of volatile organic compounds (VOCs) and non-invasive diseases diagnosis. *Carbon,* 110: 97-129.
10. Ghimenti, S., Francesco, F. Di, Onor, M., Pleil, J. D., Stiegel, M. A., Sobus, J. R., Unterkofler, K., King, J., Mochalski, P., Pleil, J. D., Stiegel, M. A. and Risby, T. H. (2013), Clinical breath analysis : discriminating between human endogenous compounds and exogenous (environmental) chemical confounder. *Journal of Breath Research,* 7: 1-11.
11. Gaude, E., Nakhleh, M. K., Patassini, S., Boschmans, J., Allsworth, M., Boyle, B., and Van Der Schee, M. P. (2019), Targeted breath analysis: Exogenous volatile organic compounds (EVOC) as metabolic pathway-specific probe. *Journal of Breath Research,* 13(3): 032001.
12. Yakin, F. S. M., Abdullah, M. F., Badaruddin, S. A, Syono, M. I. and Soriadi, N. (2021), Surface modification and properties modulation of rGO film by short duration H_2 and NH_3 plasma treatment. *Materials Today: Proceedings,* 42: 2996-3001.
13. Tombel, N. S. M., Badaruddin, S. A. M., Yakin, F. S. M., Zaki, H. F. M. and Syono, M. I. (2021). Detection of low PPM of volatile organic compounds using nanomaterial functionalized reduced graphene oxide sensor. *AIP Conference Proceedings,* 2368: 020004.
14. Amiri, V., Roshan, H., Mirzaei, A., Neri, G. and Ayesh, A. I. (2020). Nanostructured metal oxide-based acetone gas sensors : a review. *Sensors,* 20: 3096.
15. Wang, C., Yin, L., Zhang, L., Xiang, D. and Gao, R. (2010). Metal oxide gas sensors: Sensitivity and influencing factors. *Sensors,* 10: 2088-2106.
16. Aniq, M., Mohammad, S., Wah, H., Bien, D. C. S., Hj, I., Azid, A., Woon, M. and Shukri, S. (2014). Surface morphology, resistivity, and magnetoresistance of Co, Fe, Ni, Co – Fe and Ni – Fe nanoparticles on TiN layers induced by hydrogen plasma treatment. *Thin Solid Films,* 550: 22-26.
17. Arun, K., Lekshmi, M. S and Suja, K. (2021). Performance analysis, modeling, and development of a signal conditioning unit of n-type metal oxide gas sensor for acetone gas detection. *Journal of Computational Electronics,* 20: 1938-1947.
18. Arshak, K., Moore, E., Lyons, G.M., Harris, J. and Clifford, S. (2004). A review of gas sensors employed in electronic nose applications. *Sensor Review,* 24: 181-198.
19. Vergara, A., Vembu, S., Ayhan, T., Ryan, M. A., Homer, M. L. and Huerta, R. (2012). Chemical gas sensor drift compensation using classifier ensembles. *Sensors and Actuators, B: Chemical,* 166-167: 320-329.
20. Gupta, S., Chatterjee, S., Ray, A. K. and Chakraborty, A. K. (2015). Graphene – metal oxide nanohybrids for toxic gas sensor : A review. *Sensors & Actuators: B Chemical,* 221(2): 1170-1181.
21. Zhou, C., Yu, J., Qin, Y. and Zheng, J. (2013). Grain size effects in polycrystalline gold nanoparticles. *Nanoscale,* 4(14): 4228-4233.